New Power Source from Fractional Rydberg States of Atomic Hydrogen

R. L. Mills, P. Ray, B. Dhandapani, M. Nansteel, X. Chen, J. He
BlackLight Power, Inc.
493 Old Trenton Road
Cranbury, NJ 08512

ABSTRACT

Extreme ultraviolet (EUV) spectroscopy was recorded on microwave discharges of helium with 2% hydrogen. Novel emission lines were observed with energies of $q \cdot 13.6\ eV$ where $q = 1,2,3,4,6,7,8,9,11$ or these lines inelastically scattered by helium wherein $21.2\ eV$ was absorbed in the excitation of $He\ (1s^2)$ to $He\ (1s^1 2p^1)$. The average hydrogen atom temperature was measured to be 180 - 210 eV versus $\approx 3\ eV$ for pure hydrogen. The electron temperature T_e for helium-hydrogen was 28,000 K compared to 6800 K for pure helium. With a microwave input power of 40 W, the gas temperature of the plasma was measured to be 1200°C after 150 s compared to 185°C for helium alone.

1. Introduction

J. R. Rydberg showed that all of the spectral lines of atomic hydrogen were given by a completely empirical relationship:

$$\bar{\nu} = R\left(\frac{1}{n_f^2} - \frac{1}{n_i^2}\right) \tag{1}$$

where $R = 109{,}677\ cm^{-1}$, $n_f = 1,2,3,...$, $n_i = 2,3,4,...$ and $n_i > n_f$. Bohr, Schrödinger, and Heisenberg each developed a theory for atomic hydrogen that gave the energy levels in agreement with Rydberg's equation.

$$E_n = -\frac{e^2}{n^2 8\pi\varepsilon_o a_H} = -\frac{13.598\ eV}{n^2} \tag{2a}$$

$$n = 1,2,3,... \tag{2b}$$

The excited energy states of atomic hydrogen are given by Eq. (2a) for $n > 1$ in Eq. (2b). The $n = 1$ state is the "ground" state for "pure" photon transitions (i.e. the $n = 1$ state can absorb a photon and go to an excited electronic state, but it cannot release a photon and go to a lower-energy electronic state). However, an electron transition from the ground state to a lower-energy state may be possible by a resonant nonradiative energy transfer such as multipole coupling or a resonant collision mechanism. Processes such as hydrogen molecular bond formation that occur without photons and that require collisions are common [1]. Also, some commercial phosphors are based on resonant nonradiative energy transfer involving multipole coupling [2].

We propose that atomic hydrogen may undergo a catalytic reaction with certain atoms and ions such as He^+ which singly or multiply ionize at integer multiples of the potential energy of atomic hydrogen, $m \cdot 27.2\ eV$ wherein m is an integer. The theory was given previously [3-5]. The reaction involves a nonradiative energy transfer to form a hydrogen atom that is lower in energy than unreacted atomic hydrogen that corresponds to a fractional principal quantum number. That is

$$n = \frac{1}{2}, \frac{1}{3}, \frac{1}{4}, ..., \frac{1}{p};\quad p \text{ is an integer} \tag{2c}$$

replaces the well known parameter $n = \text{integer}$ in the Rydberg equation for hydrogen excited states. The $n = 1$ state of hydrogen and the $n = \frac{1}{\text{integer}}$

states of hydrogen are nonradiative, but a transition between two nonradiative states is possible via a nonradiative energy transfer, say $n=1$ to $n=1/2$. Thus, a catalyst provides a net positive enthalpy of reaction of $m \cdot 27.2\ eV$ (i.e. it resonantly accepts the nonradiative energy transfer from hydrogen atoms and releases the energy to the surroundings to affect electronic transitions to fractional quantum energy levels). As a consequence of the nonradiative energy transfer, the hydrogen atom becomes unstable and emits further energy until it achieves a lower-energy nonradiative state having a principal energy level given by Eqs. (2a) and (2c).

Prior related studies that support the possibility of a novel reaction of atomic hydrogen which produces hydrogen in fractional quantum states that are at lower energies than the traditional "ground" ($n=1$) state include EUV spectroscopy [6-12], characteristic emission from catalysts and the hydride ion products [8], lower-energy hydrogen emission [6-8, 12], chemically formed plasmas [8-11], Balmer α line broadening [12-13], anomalous plasma afterglow duration [11], power generation [9, 13-14], and analysis of novel chemical compounds [15]. We report that microwave discharges of helium-hydrogen mixtures were studied by EUV spectroscopy to search for line emission from transitions to fractional Rydberg states of atomic hydrogen. Since the electronic transitions are very energetic, Balmer α line broadening, electron temperature, and the gas temperature were measured.

2. Experimental

EUV spectroscopy was recorded on hydrogen, xenon, helium, xenon-hydrogen (98/2%), and helium-hydrogen (98/2%) microwave discharge plasmas (Frequency: 2450 MHz) according to the methods given previously [6]. A xenon-hydrogen (98/2%) or helium-hydrogen (98/2%) gas mixture was flowed at 1 Torr or 20 Torr through a half inch diameter quartz tube fitted with an Evenson cavity, and each plasma of hydrogen, xenon, and helium alone was run at 20 Torr. The input power to the plasma was set at 85 W with forced air cooling of the cell. The spectrometer was a normal incidence 0.2 m monochromator equipped with a 1200 lines/mm holographic grating with a platinum coating that

covered the region $2-560\,nm$. The EUV spectrum was recorded with a CEM. The wavelength resolution was about $0.02\,nm$ (FWHM) with slit widths of $50\,\mu m$. The increment was $0.2\,nm$ and the dwell time was $500\,ms$. Peak assignments were based on a calibration against the known He I and He II lines.

To achieve higher sensitivity at the shorter EUV wavelengths, the light emission from plasmas of helium alone was recorded with a 4° grazing incidence EUV spectrometer equipped with a grating having 600 G/mm with a radius of curvature of $\approx 1\,m$ that covered the region $5-65\,nm$. The angle of incidence was 87°. The resolution was about $0.04\,nm$ (FWHM) with slit widths of $300\,\mu m$. A CEM was used to detect the EUV light. The increment was $0.1\,nm$ and the dwell time was $1\,s$.

The width of the 656.2 nm Balmer α line emitted from hydrogen alone, xenon-hydrogen mixture (90/10)%, and helium-hydrogen mixture (90/10)% microwave discharge plasmas was measured with a high resolution visible spectrometer capable of a resolution of $\pm 0.006\,nm$ [16]. In this case, the total pressure was 1 Torr, and the input power to the plasma was set at 40 W.

T_e was measured on 0.1 Torr microwave plasmas of helium alone and helium-hydrogen mixtures (90/10%) from the ratio of the intensity of the *He* 501.6 nm (upper quantum level n=3) line to that of the *He* 492.2 nm (n=4) line as described by Griem [17]. T_e was measured on hydrogen alone plasmas from their Balmer line intensities. The visible spectrum $400-560\,nm$ was recorded with the normal incidence EUV spectrometer using a PMT and a sodium salicylate scintillator.

In order to estimate the power of the cell as described previously [18], the gas temperature of microwave plasmas of helium and xenon alone and each noble gas with 10% hydrogen was recorded using a K-type thermocouple ($\pm 0.1\,°C$) housed in a stainless steel tube that was placed axially inside the center of the 10 cm^3 plasma volume of the quartz microwave cell. At 40 W input with forced air cooling, the temperature rise was measured for 150 s then stopped, and the cooling curve was measured. The pressure of the ultrahigh pure gas inside the cell was maintained at about 300 mTorr with a noble gas flow rate of 9.3 sccm or a noble gas flow rate of 8.3 sccm and a hydrogen flow rate of 1 sccm controlled by a mass flow controller.

3. Results and discussion

A. EUV Spectroscopy

In the case of the EUV spectrum of hydrogen, xenon, or xenon-hydrogen (98/2%), no peaks were observed below 78 *nm*, and no spurious peaks or artifacts due to the grating or the spectrometer were observed. Only known He I and He II peaks were observed in the EUV spectrum of the control helium microwave discharge cell emission.

The EUV spectra (17.5 – 50 *nm*) of the microwave cell emission of the helium-hydrogen mixture (98/2%) (top curve) and the helium control (bottom curve) are shown in Figure 1. Ordinary hydrogen has no emission in these regions. Novel peaks were observed at 45.6 *nm*, 37.4 *nm*, and 20.5 *nm* which do not correspond to helium. At the 1 Torr condition, additional novel peaks were observed in the short wavelength region (5 – 65 *nm*) at 14.15 *nm*, 13.03 *nm*, 10.13 *nm*, and 8.29 *nm* which do not correspond to helium as shown in Figure 1. Known He I lines which were used for calibration of the novel peak positions were observed at 58.4 *nm*, 53.7 *nm*, and 52.4 *nm*. It is proposed that the 30.4 *nm* peak shown in Figures 1 and 2 was not entirely due to the He II transition. In the case of the helium-hydrogen mixture, the ratio of 30.4 *nm* (40.8 *eV*) peak to the 25.6 *nm* (48.3 *eV*) was 10 compared to 5.4 for helium alone as shown in Figure 1 which implies only a minor He II transition contribution to the 30.4 *nm* peak.

It is proposed that the majority of the 91.2 *nm* peak was also due to a novel transition. At 20 Torr, the ratio of the Lyman β peak to the 91.2 *nm* peak of the helium-hydrogen plasma was 2 compared to 8 for each control hydrogen and xenon-hydrogen plasma which indicates that the majority of the 91.2 *nm* peak was due to a transition other than the binding of an electron by a proton.

The novel peaks fit two empirical relationships. In order of energy, the set comprising the peaks at 91.2 *nm*, 45.6 *nm*, 30.4 *nm*, 13.03 *nm*, 10.13 *nm*, and 8.29 *nm* correspond to energies of $q \cdot 13.6\ eV$ where $q = 1,2,3,7,9,11$. In order of energy, the set comprising the peaks at 37.4 *nm*, 20.5 *nm*, and 14.15 *nm* correspond to energies of $q \cdot 13.6 - 21.21\ eV$ where $q = 4,6,8$. These

lines can be explained as electronic transitions to fractional Rydberg states of atomic hydrogen given by Eqs. (2a) and (2c) wherein the catalytic system involves helium ions because the second ionization energy of helium is $54.417\,eV$, which is equivalent to $2 \cdot 27.2\,eV$. In this case, $54.417\,eV$ is transferred nonradiatively from atomic hydrogen to He^+ which is resonantly ionized. The electron decays to the $n = 1/3$ state with the further release of $54.417\,eV$ which may be emitted as a photon. The catalysis reaction is

$$54.417\,eV + He^+ + H[a_H] \rightarrow He^{2+} + e^- + H\left[\frac{a_H}{3}\right] + 108.8\,eV \tag{3}$$

$$He^{2+} + e^- \rightarrow He^+ + 54.417\,eV \tag{4}$$

And, the overall reaction is

$$H[a_H] \rightarrow H\left[\frac{a_H}{3}\right] + 54.4\,eV + 54.4\,eV \tag{5}$$

Since the products of the catalysis reaction have binding energies of $m \cdot 27.2\,eV$, they may further serve as catalysts. Thus, further catalytic transitions may occur: $n = \frac{1}{3} \rightarrow \frac{1}{4}$, $\frac{1}{4} \rightarrow \frac{1}{5}$, and so on.

Electronic transitions to Rydberg states given by Eqs. (2a) and (2c) catalyzed by the resonant nonradiative transfer of $m \cdot 27.2\,eV$ would give rise to a series of emission lines of energies $q \cdot 13.6\,eV$ where q is an integer. It is further proposed that the photons that arise from hydrogen transitions may undergo inelastic helium scattering. That is, the catalytic reaction

$$H[a_H] \xrightarrow{He} H\left[\frac{a_H}{3}\right] + 54.4\,eV + 54.4\,eV \tag{6}$$

yields $54.4\,eV$ by Eq. (4) and a photon of $54.4\,eV$ ($22.8\,nm$). Once emitted, the photon may be absorbed or scattered. When this photon strikes $He(1s^2)$, $21.2\,eV$ may be absorbed in the excitation to $He(1s^1 2p^1)$. This leaves a $33.19\,eV$ ($37.4\,nm$) photon peak and a $21.2\,eV$ ($58.4\,nm$) photon from $He(1s^1 2p^1)$. Thus, for helium the inelastic scattered peak of $54.4\,eV$ photons from Eq. (3) is given by

$$E = 54.4\,eV - 21.21\,eV = 33.19\,eV\ (37.4\,nm) \tag{7}$$

A novel peak shown in Figures 1 and 2 was observed at $37.4\,nm$. Furthermore, the intensity of the $58.4\,nm$ peak corresponding to the spectra shown in Figure 2 was about 60,000 photons/sec. Thus, the transition $He(1s^2) \rightarrow He(1s^1 2p^1)$ dominated the inelastic scattering of EUV

peaks. The general reaction is

$$photon\,(h\nu) + He\,(1s^2) \rightarrow He\,(1s^1 2p^1) + photon\,(h\nu - 21.21\,eV) \quad (8)$$

The two empirical series may be combined—one directly from Eqs. (2a, 2c) and the other indirectly with Eq. (8). The energies for the novel lines in order of energy are $13.6\,eV$, $27.2\,eV$, $40.8\,eV$, $54.4\,eV$, $81.6\,eV$, $95.2\,eV$, $108.8\,eV$, $122.4\,eV$ and $149.6\,eV$. The corresponding peaks are $91.2\,nm$, $45.6\,nm$, $30.4\,nm$, $37.4\,nm$, $20.5\,nm$, $13.03\,nm$, $14.15\,nm$, $10.13\,nm$, and $8.29\,nm$, respectively. Thus, the identified novel lines correspond to energies of $q \cdot 13.6\,eV$ where $q = 1,2,3,4,6,7,8,9,11$ or these lines inelastically scattered by helium atoms wherein $21.2\,eV$ was absorbed in the excitation of $He\,(1s^2)$ to $He\,(1s^1 2p^1)$. The values of q observed are consistent with those excepted based on Eq. (5) and the subsequent autocatalyzed reactions as discussed previously [6]. The satellite peak at $44.2\,nm$ show in Figure 1 and 2 may be due to multipole coupling as discussed elsewhere [12]. There is remarkable agreement between the data and the proposed transitions to fractional Rydberg states and these lines inelastically scattered by helium according to Eq. (8). All other peaks could be assigned to He I, He II, second order lines, or atomic or molecular hydrogen emission. No known lines of helium or hydrogen explain the $q \cdot 13.6\,eV$ related set of peaks.

Since its ionization energy is $27.63\,eV$, Ar^+ may also serve as a catalyst by providing a net enthalpy of an integer multiple of the potential energy of atomic hydrogen. In recent argon-hydrogen plasma experiments, to be reported, lines with energies of $q \cdot 13.6\,eV$ where $q = 7,9,11$ were observed without the lines assigned in Figures 1-2 to helium inelastic scattering. This supports the present assignment of the helium scattered lines. Furthermore, hydrogen scattered lines were not expected since the gas was helium-hydrogen (98/2%).

B. Line broadening and T_r measurements

The Doppler-broadened line shape for atomic hydrogen has been studied on many sources such as hollow cathode [19-20] and rf [21-22] discharges. The method of Videnocic et al. [19] was used to calculate the energetic hydrogen atom densities and energies from the width of the 656.2 nm Balmer α line emitted from the hydrogen and helium-hydrogen mixture (90/10%) microwave plasmas shown in Figure 3.

Gigosos et al. [23] have reviewed the literature and have discussed the limitations of this method. The average helium-hydrogen Doppler half-width of $0.52 \pm 5\%\ nm$ was not appreciably changed with pressure. The corresponding energy of $180\text{-}210\ eV$ and the number densities of $5 X 10^{14} \pm 20\%\ atoms/cm^3$, depending on the pressure, were significant compared to only $\approx 3\ eV$ and $7 X 10^{13}\ atoms/cm^3$ for pure hydrogen even though 10 times more hydrogen was present. Only $\approx 3\ eV$ broadening was observed with xenon-hydrogen (98/2%) ruling out collisional broadening.

Similarly, the average electron temperature for helium-hydrogen plasma was $28{,}000 \pm 5\%\ K$. Whereas, the corresponding temperature of helium alone was only $6800 \pm 5\%\ K$, and hydrogen alone was $5500 \pm 5\%\ K$. No high electric field was present in our experiments. Thus, the results can not be explained by Stark broadening or acceleration of charged species due to high fields of over $10\ kV/cm$ as proposed by Videnocic et al. [19] to explain excessive broadening observed in glow discharges.

C. Gas temperature measurements

No increase in temperature was observed with the addition of hydrogen to xenon control. In contrast, the plasma gas temperature increased from room temperature to 1200°C within 150 seconds for helium-hydrogen compared to only 185°C for helium alone as shown in Figure 4.

A conservative estimate of the total output power was determined by taking the ratio of the areas of the helium-hydrogen temperature-rise-above-ambient-versus-time curve compared to that of helium only, 10, multiplied by the common input. Thus, with a microwave input power of $40\ W$, the thermal output power was estimated to be $400\ W$. A second estimate of the power from the $10\ cm^3$ plasma volume based on the Stefan-Boltzmann equation using an emissivity of 0.5 and a measured wall temperature of 1200°C was at least $400\ W$. Since the hydrogen flow rate was 1 sccm, an estimate of the corresponding energy balance was over $-5 X 10^5\ kJ/mole\ H_2$ compared to the enthalpy of combustion of hydrogen of $-241.8\ kJ/mole\ H_2$.

4. Conclusion

We report that novel emission lines were observed with energies of $q \cdot 13.6\,eV$ where $q = 1,2,3,4,6,7,8,9,11$ or these lines inelastically scattered by helium atoms wherein $21.2\,eV$ was absorbed in the excitation of $He(1s^2)$ to $He(1s^1 2p^1)$. These lines were identified as transitions to fractional Rydberg states of atomic hydrogen. An extremely high hydrogen-atom temperature of $180\text{-}210\,eV$ was observed with the presence of helium ion catalyst only with hydrogen also present. Similarly, the average electron temperature for helium-hydrogen plasma was high, 28,000 K, compared to 6800 K for helium alone. An estimate of the thermal power was $400\,W$ in $10\,cm^3$.

Acknowledgments

Special thanks to Y. Lu and T. Onuma for recording some spectra. We thank one of the referees for useful suggestions. Detailed differential energy balances and the ToF measurement of He^{2+} by Eq. (3) will be pursued.

References

[1] N. V. Sidgwick, *The Chemical Elements and Their Compounds*, Volume I, Oxford, Clarendon Press, (1950), p.17.

[2] M. D. Lamb, *Luminescence Spectroscopy*, Academic Press, London, (1978), p. 68.

[3] R. Mills, *The Grand Unified Theory of Classical Quantum Mechanics*, September 2001 Edition, BlackLight Power, Inc., Cranbury, New Jersey, Distributed by Amazon.com; posted at www.blacklightpower.com.

[4] R. Mills, Int. J. Hydrogen Energy, in press.

[5] R. Mills, Int. J. Hydrogen Energy, Vol. 26, No. 10, (2001), pp. 1059-1096.

[6] R. Mills, P. Ray, Int. J. Hydrogen Energy, in press.

[7] R. Mills, P. Ray, Int. J. Hydrogen Energy, in press.

[8] R. Mills, Int. J. Hydrogen Energy, Vol. 26, No. 10, (2001), pp. 1041-1058.

[9] R. Mills, M. Nansteel, and Y. Lu, Int. J. Hydrogen Energy, Vol. 26, No. 4, (2001), pp. 309-326.
[10] R. Mills, J. Dong, Y. Lu, Int. J. Hydrogen Energy, Vol. 25, (2000), pp. 919-943.
[11] R. Mills, T. Onuma, and Y. Lu, Int. J. Hydrogen Energy, Vol. 26, No. 7, July, (2001), pp. 749-762.
[12] R. L. Mills, P. Ray, B. Dhandapani, J. He, J. of Phys. Chem., submitted.
[13] R. Mills, A. Voigt, P. Ray, M. Nanstell, Int. J. Hydrogen Energy, in press.
[14] R. Mills, N. Greenig, S. Hicks, Int. J. Hydrogen Energy, in press.
[15] R. Mills, B. Dhandapani, M. Nansteel, J. He, T. Shannon, A. Echezuria, Int. J. of Hydrogen Energy, Vol. 26, No. 4, (2001), pp. 339-367.
[16] R. L. Mills, P. Ray, B. Dhandapani, J. He, Chem. Phys., submitted.
[17] H. R. Griem, *Principle of Plasma Spectroscopy*, Cambridge University Press, (1987).
[18] C. Chen, T. Wei, L. R. Collins, J. Phillips, J. Phys. D: Appl. Phys., Vol. 32, (1999), pp. 688-698.
[19] I. R. Videnocic, N. Konjevic, M. M. Kuraica, Spectrochimica Acta, Part B, Vol. 51, (1996), pp. 1707-1731.
[20] S. Alexiou, E. Leboucher-Dalimier, Phys, Rev. E, Vol. 60, No. 3, (1999), pp. 3436-3438.
[21] S. Djurovic, J. R. Roberts, J. Appl. Phys., Vol. 74, No. 11, (1993), pp. 6558-6565.
[22] S. B. Radovanov, K. Dzierzega, J. R. Roberts, J. K. Olthoff, Appl. Phys. Lett., Vol. 66, No. 20, (1995), pp. 2637-2639.
[23] M. A. Gigosos, V. Cardenoso, J. Phys. B: At. Mol. Opt. Phys., Vol. 29, (1996), pp. 4795-4838.

Figure Captions

Figure 1. The EUV spectra (17.5 – 50 *nm*) of the microwave cell emission of the helium-hydrogen mixture (98/2%) (top curve) recorded at 20 Torr with a normal incidence EUV spectrometer and a CEM, and control helium (bottom curve) recorded at 20 Torr with a 4° grazing incidence EUV spectrometer and a CEM. Only known He I and He II peaks were observed with the helium control. Reproducible novel emission lines were observed at 45.6 *nm* and 30.4 *nm* with energies of $q \cdot 13.6\,eV$ where $q = 2\ or\ 3$ (Eqs. (2a, 2c)) and at 37.4 *nm* and 20.5 *nm* with energies of $q \cdot 13.6\,eV$ where $q = 4\ or\ 6$ that were inelastically scattered by helium atoms wherein 21.2 *eV* was absorbed in the excitation of $He\,(1s^2)$ to $He\,(1s^1 2p^1)$ as proposed in Eq. (8).

Figure 2. The short wavelength EUV spectra (5 – 65 *nm*) of the microwave cell emission of the helium-hydrogen mixture (98/2%) (top curve) and control hydrogen (bottom curve) recorded at 1 Torr with a normal incidence EUV spectrometer and a CEM. No hydrogen emission was observed in this region, and no instrument artifacts were observed. Reproducible novel emission lines were observed at 45.6 *nm*, 30.4 *nm*, 13.03 *nm*, 10.13 *nm*, and 8.29 *nm* with energies of $q \cdot 13.6\,eV$ where $q = 2,3,7,9,\ or\ 11$ and at 37.4 *nm*, 20.5 *nm*, and 14.15 *nm* with energies of $q \cdot 13.6\,eV$ where $q = 4,6,\ or\ 8$ that were inelastically scattered by helium atoms wherein 21.2 *eV* was absorbed in the excitation of $He\,(1s^2)$ to $He\,(1s^1 2p^1)$ as proposed in Eq. (8).

Figure 3. The 656.2 nm Balmer α line width recorded with a high resolution (±0.006 *nm*) visible spectrometer on a helium-hydrogen (90/10%) and a hydrogen microwave discharge plasma. Significant broadening was observed corresponding to an average hydrogen atom temperature of 180 - 210 *eV*.

Figure 4. The plasma gas temperature rise as a function of time for helium alone and the helium-hydrogen mixture (90/10%) with microwave input power set at 40 W. The maximum temperature of the helium-hydrogen mixture and the helium alone plasma was 1200°C and 185°C, respectively. The thermal output power of the helium-hydrogen plasma was estimated to be 400 *W*.

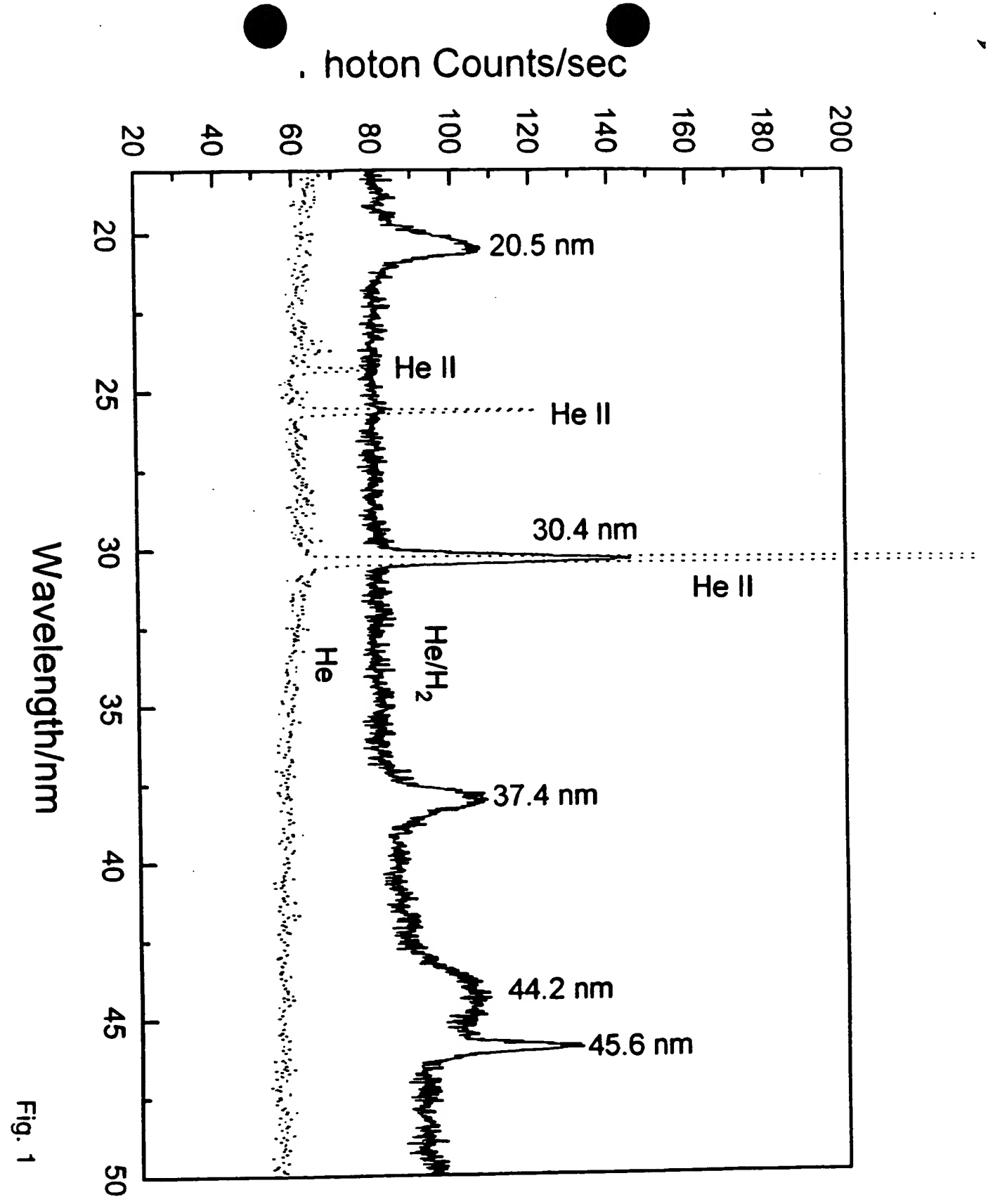
. hoton Counts/sec
20
40
60
80
100
120
140
160
180
200
Wavelength/nm
20
25
30
35
40
45
50
20.5 nm
He II
He II
30.4 nm
He II
He
He/H2
37.4 nm
44.2 nm
45.6 nm

Fig. 1

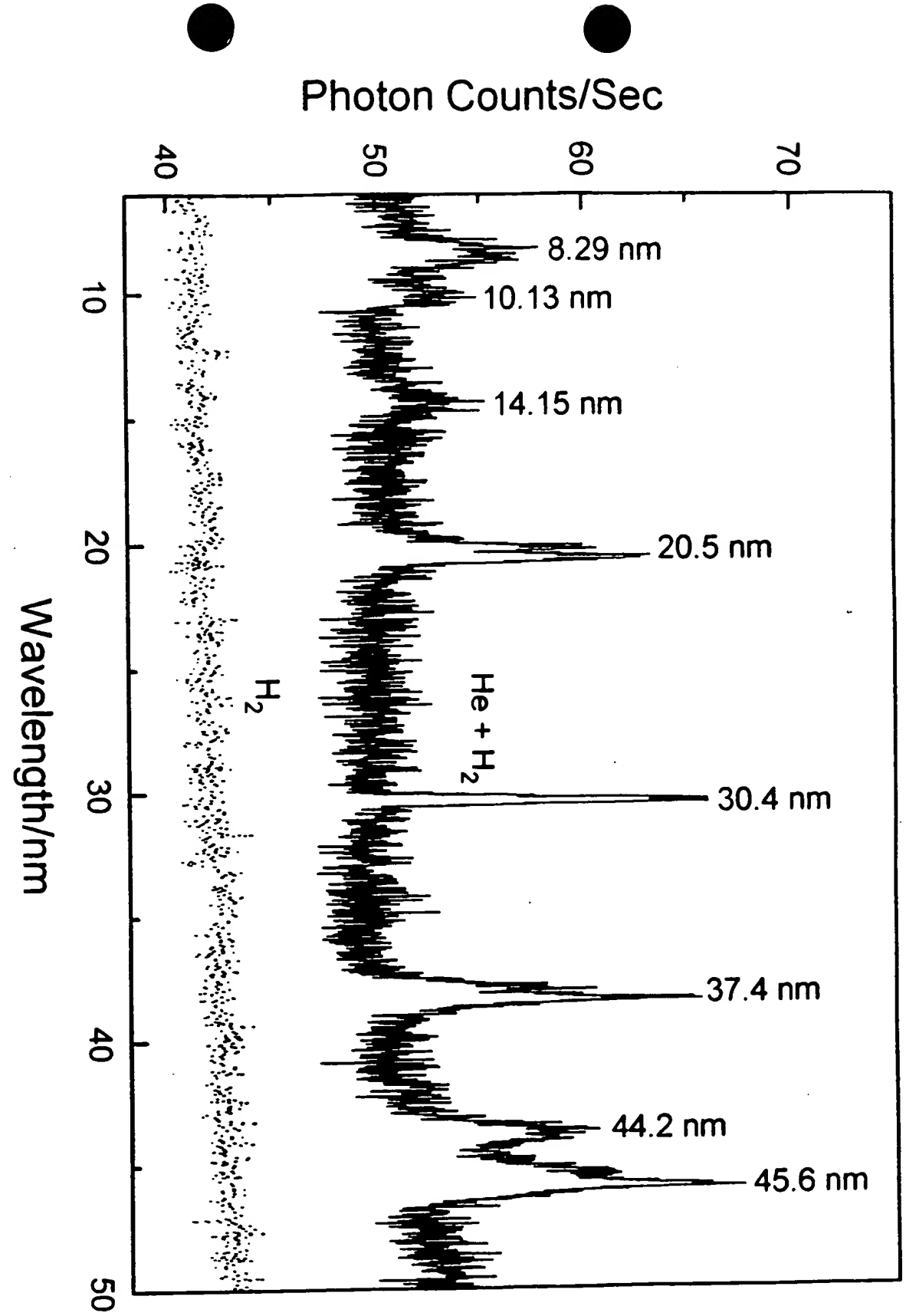
Photon Counts/Sec
40
50
60
70
Wavelength/nm
10
20
30
40
50
8.29 nm
10.13 nm
14.15 nm
20.5 nm
30.4 nm
37.4 nm
44.2 nm
45.6 nm
H2
He + H2

Fig. 2

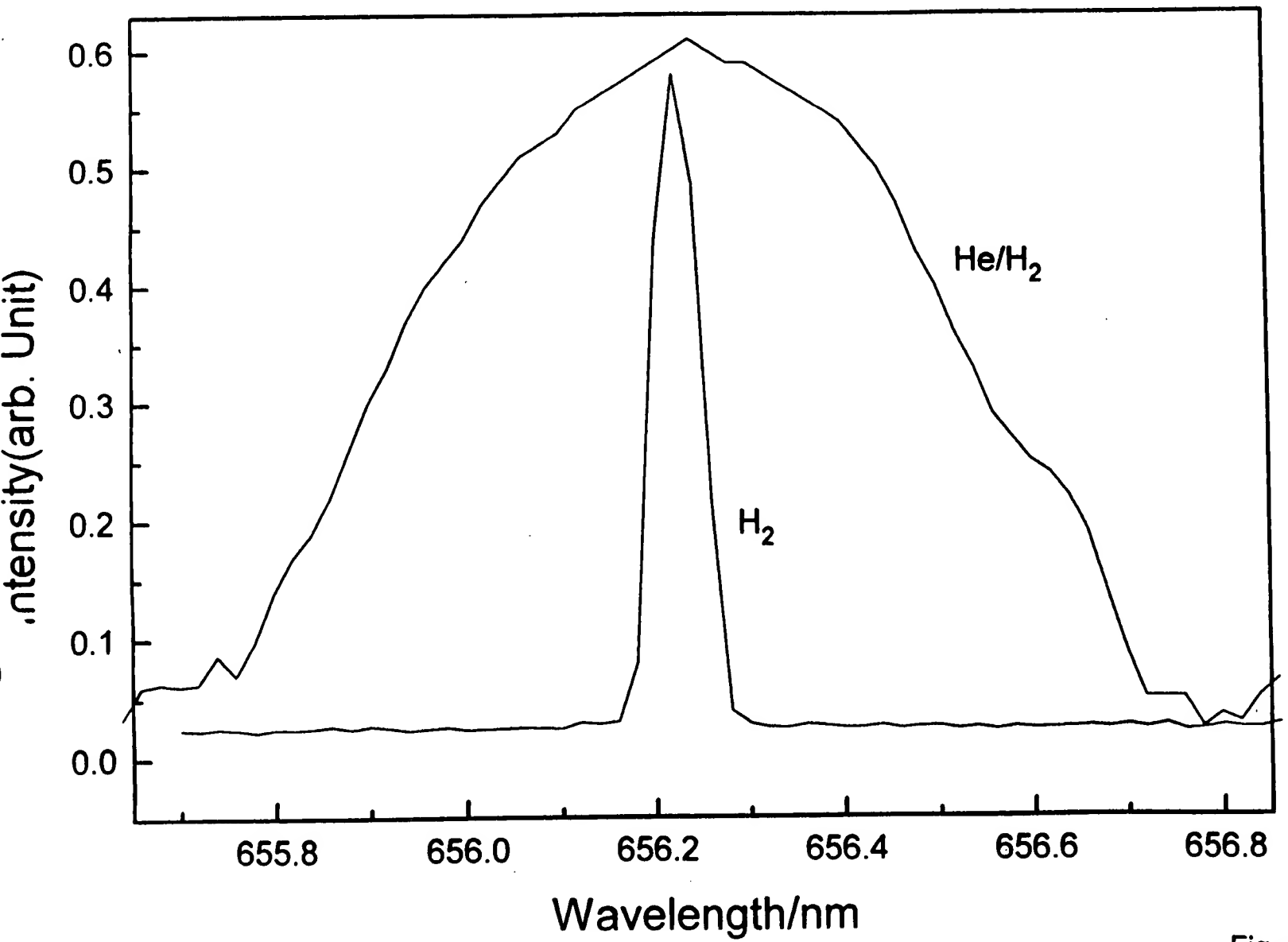
0.6
0.5
0.4
0.3
0.2
0.1
0.0
ntensity(arb. Unit)
He/H2
H2
655.8
656.0
656.2
656.4
656.6
656.8
Wavelength/nm

Fig. 3

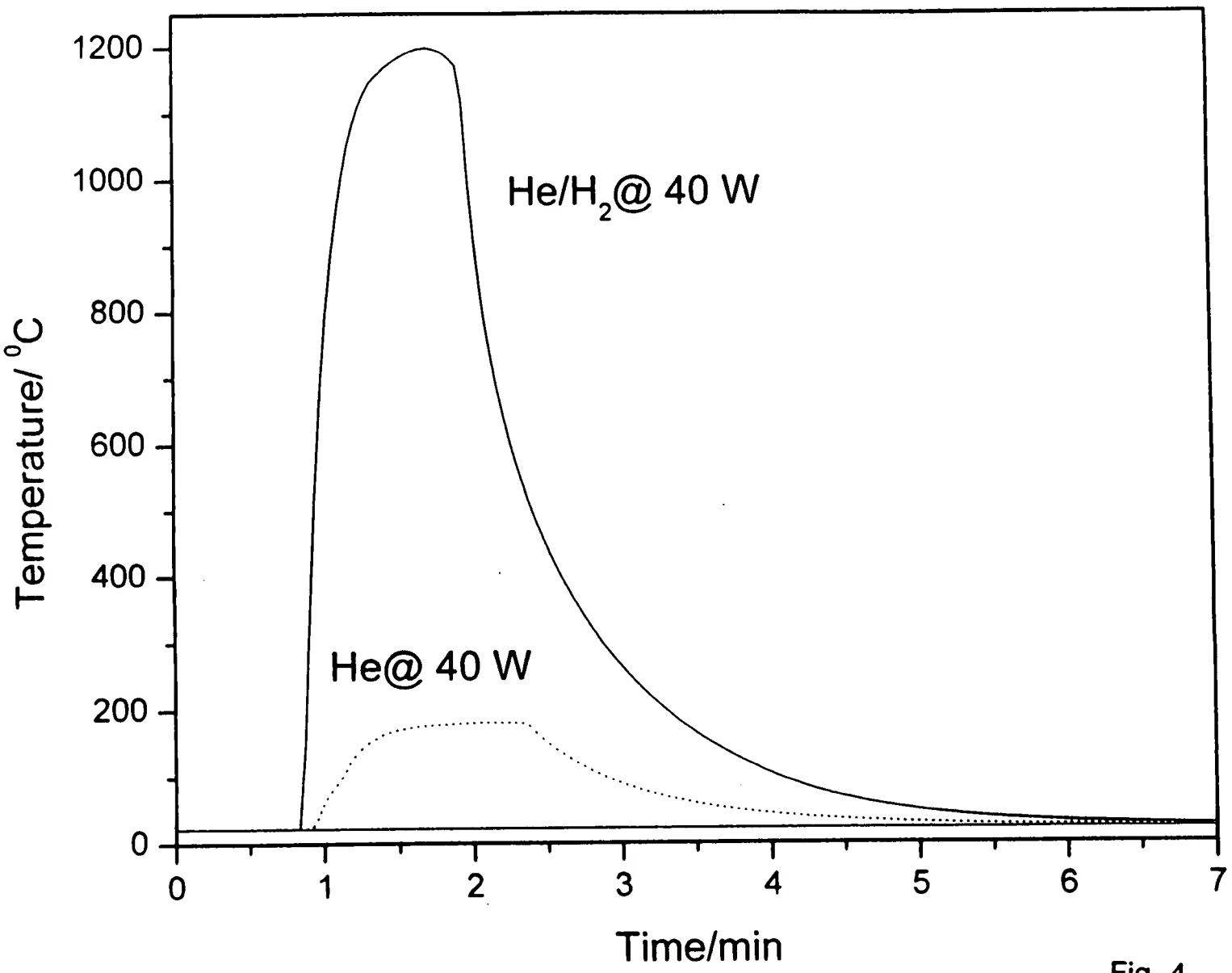
1200
1000
800
600
400
200
0
Temperature/ °C
He/H2@ 40 W
He@ 40 W
0
1
2
3
4
5
6
7
Time/min

Fig. 4